

NIKHEF/2012-007
 ITP-UU-12/12
 IMSc 2012/4/6
 FR-PHENO-2012-006

Soft-collinear effects for prompt photon production via fragmentation

Rahul Basu^{a†}, Eric Laenen^b, Anuradha Misra^c, Patrick Motylinski^d

^a The Institute of Mathematical Sciences, CIT Campus, Taramani, Chennai 600 113, India

^bITFA, Science Park 904, 1090 GL Amsterdam,
 ITF, Utrecht University, Leuvenlaan 4, 3584 CE Utrecht
 Nikhef, Science Park 105, 1098 XG Amsterdam, The Netherlands

^c Department of Physics, University of Mumbai, Santacruz(E), Mumbai, 400 098, India

^d Physikalisches Institut, Albert-Ludwigs-Universität Freiburg, Hermann-Herder-Straße 3,
 D-79104 Freiburg i.Br., Germany

This paper is dedicated to the memory of Rahul Basu.

Abstract

We study the impact of leading soft-collinear effects on threshold and joint-resummed calculations for the production of prompt photons via parton fragmentation, complementing a previous study for direct production. We assess these effects for both fixed-target and collider kinematics. We find them to be small, but noticeable and comparable to the direct case.

[†]Deceased.

1 Introduction

The perturbative QCD description of prompt production at hadron colliders can involve sizeable corrections from soft and collinear parton emission. In particular, the presence of a threshold at fixed p_T induces large logarithmic corrections [1, 2]. Expressed in terms of a (Mellin) moment variable N with the property that as $N \rightarrow \infty$ the kinematics approaches the threshold limit, these corrections take the form ($L = \ln N$),

$$\alpha_s^i \sum_j^{2i} a_{ij} L^j, \quad (1)$$

where the a_{ij} depend in general on the process. Such large logarithmic corrections can be organized and controlled through all-order resummation, for threshold [3–8] and joint [9–13] resummation.

In recent years, in the context of threshold resummation, other large classes of terms have been brought under all-order control, such as large constants (“ π^2 terms”) [14–16] and a series of so-called “soft-collinear” terms

$$\alpha_s^i \sum_j^{2i-1} d_{ij} \frac{\ln^j N}{N}. \quad (2)$$

In a previous study [17] we performed the resummation of the leading terms ($j = 2i - 1$) for direct production of prompt photons. In this paper we extend this study to the leading soft-collinear terms (which we shall also refer to as “ $\ln N/N$ terms”) in the complimentary case of prompt photon production by fragmentation. In this case more subprocesses contribute, and their color states must be accounted for. These issues occur as well in threshold resummation without soft-collinear effects for both mechanisms of prompt photon production [18]. Subleading soft-collinear terms have been studied recently in other contexts in Refs. [19–31].

The paper is organized as follows. In section 2 we review briefly the threshold and joint resummed prompt photon p_T distribution, and discuss the inclusion of soft-collinear effects. In section 3 we assess the numerical impact of these corrections, and we conclude in section 4. In three appendices we clarify various technical points.

2 Resummed transverse momentum distributions

We consider the inclusive transverse momentum distribution of prompt photons produced at fixed p_T in hadron-hadron collisions at center of mass (cm) energy \sqrt{S}

$$h_A(p_A) + h_B(p_B) \rightarrow \gamma(p_c) + X, \quad (3)$$

where $h_{A,B}$ refers to the two incoming hadrons and X to the unobserved part of the final state. The lowest order QCD processes producing the prompt photon directly at partonic cm energy \sqrt{s} are

$$\begin{aligned} q(p_a) + \bar{q}(p_b) &\rightarrow \gamma(p_c) + g(p_d) \\ g(p_a) + q(p_b) &\rightarrow \gamma(p_c) + q(p_d), \end{aligned} \quad (4)$$

where in the second reaction q stands for both quark and anti-quark. The minimum invariant mass s required for the final state is $4p_T^2$. It is convenient to express the distance above

threshold by the variable $1 - x_T^2$, where $x_T^2 = 4p_T^2/S$. At the parton level this becomes $1 - \hat{x}_T^2 = 1 - 4p_T^2/s$.

Apart from the partonic sub processes that directly produce the photon, there are contributions from $2 \rightarrow 2$ parton scattering

$$a(p_a) + b(p_b) \rightarrow c(p_c) + d(p_d), \quad (5)$$

where the photon is produced by fragmentation of final state parton c . In this paper, given the accuracy to which we work, this will be either a quark or anti-quark. The fragmentation component also contributes at $O(\alpha\alpha_s)$, as does the direct component, though it is subdominant in the sense that the fragmentation function behaves as $1/N$ [5]. This is in part because, for pp and pN collisions, the fragmentation component proceeds via valence quark scattering, as opposed to direct component which involves either a gluon or a sea quark. Moreover, threshold resummation can substantially enhance this fragmentation component [18]. Here we consider the contribution of the fragmentation component to the threshold and joint-resummed cross section for prompt photons at fixed p_T when also the leading soft-collinear effects are included.

The resummed cross section consists of two parts

$$\frac{p_T^3 d\sigma_{AB \rightarrow \gamma + X}^{(\text{resum})}}{dp_T} = \frac{p_T^3 d\sigma_{AB \rightarrow \gamma + X}^{(\text{direct})}}{dp_T} + \frac{p_T^3 d\sigma_{AB \rightarrow \gamma + X}^{(\text{frag})}}{dp_T} \quad (6)$$

where the two terms correspond to the subprocesses (4) and (5), respectively.

The expression for the joint- and threshold-resummed p_T distribution of the direct component of the prompt photon hadroproduction cross section was derived in [10] (expressed in a somewhat different form in [17]). To be able to compare the expression for the fragmentation component below in Eq. (15) with that for the direct component, we quote the latter result again here, but explain its structure only briefly. To next-to-leading logarithmic accuracy, with leading $\ln N/N$ effects included, it reads

$$\begin{aligned} \frac{p_T^3 d\sigma_{AB \rightarrow \gamma + X}^{(\text{direct})}}{dp_T} &= \frac{p_T^4}{8\pi S^2} \sum_{ab} \int_C \frac{dN}{2\pi i} \int \frac{d^2 \mathbf{Q}_T}{(2\pi)^2} \int d^2 \mathbf{b} e^{i\mathbf{b} \cdot \mathbf{Q}_T} \theta(\bar{\mu} - |\mathbf{Q}_T|) \\ &\times \int_0^1 d\tilde{x}_T^2 (\tilde{x}_T^2)^N \frac{|M_{ab}(\tilde{x}_T^2)|^2}{\sqrt{1 - \tilde{x}_T^2}} C_{ab \rightarrow \gamma d}(\alpha_s(\mu), \tilde{x}_T^2) \left(\frac{S}{4|\mathbf{p}_T - \mathbf{Q}_T/2|^2} \right)^{N+1} \\ &\times \mathcal{C}_{a/A}(Q, b, N) \mathcal{C}_{b/B}(Q, b, N) \exp [E_a^{\text{PT}}(N, b, \mu, Q) + E_b^{\text{PT}}(N, b, \mu, Q)] \\ &\times \exp [F_d(N, Q, \mu) + g_{abd}^{(1)}(\lambda)] . \end{aligned} \quad (7)$$

Joint resummation resums threshold and recoil logarithms together in terms of the variable N , the Mellin conjugate to \hat{x}_T^2 , and the impact parameter \mathbf{b} , the Fourier conjugate to \mathbf{Q}_T [9, 10]. The latter is the recoil transverse momentum of the underlying hard scattering process, over which in the top line the integral is taken. The variable $\bar{\mu}$ is a cut-off on this transverse momentum. The hard scale Q is in the present case equal to $2p_T$, and μ is the renormalization scale.

The second line contains a Mellin transform over the partonic scaling variable \tilde{x}_T^2 in the recoil frame (indicated by the tilde), the Born amplitude M_{ab} , the N - and b -independent hard virtual corrections $C_{ab \rightarrow \gamma d}(\alpha_s(\mu), \tilde{x}_T^2)$ and a kinematic factor linking recoil (through \mathbf{Q}_T) and

threshold (through N) effects. Finally, the last two lines contain the Sudakov exponentials from initial and final partons as well as soft wide angle radiation in combined (N, b) space. They also feature the coefficients $\mathcal{C}_{a/A}(Q, b, N)$ and $\mathcal{C}_{b/B}(Q, b, N)$ which contain the evolution matrix for evolution of the parton distribution functions $f_{h/H}(N, \mu_F)$ from scale μ_F to scale Q/χ and the parton distribution functions.

The initial state perturbative exponent is given by

$$E_a^{\text{PT}}(N, b, Q, \mu) = \frac{1}{\alpha_s(\mu)} h_a^{(0)}(\beta) + h_a^{(1)}(\beta, Q, \mu) , \quad (8)$$

with

$$\beta = b_0 \alpha_s(\mu) \ln(\chi) . \quad (9)$$

The functions $h_a^{(0,1)}$ are listed in the Appendix A. The function $\chi(bQ, N)$ defines the N and b dependent minimum scale of soft gluons to be included. As in [17] we choose it to be

$$\chi(bQ, N) = \bar{b} + \frac{\bar{N}}{1 + \eta \bar{b}/\bar{N}} , \quad (10)$$

where

$$\bar{N} = N e^{\gamma_E} , \quad \bar{b} = b Q e^{\gamma_E} / 2 , \quad (11)$$

γ_E being the Euler constant. The functions $\mathcal{C}_{a/A}(Q, b, N)$ and $\mathcal{C}_{b/B}(Q, b, N)$ are given by

$$\mathcal{C}_{h/H}(Q, b, N) = \sum_g \mathcal{E}_{hg}(N, Q/\chi, \mu_F) f_{g/H}(N, \mu_F) . \quad (12)$$

where the matrix \mathcal{E} is the evolution matrix which implements evolution from scale μ_F to scale Q/χ . In so doing [32] one includes the leading $\ln N/N$ effects due to initial state radiation in the evolution kernel [17]. Note that, as a consequence, the expressions for $h_a^{(0)}$ and $h_a^{(1)}$ given here are slightly different from the versions in Ref. [10]. To the accuracy we work, the μ_F dependence essentially cancels in Eq. (12).

The final state exponent reads [33]

$$F_d(N, Q, \mu) \equiv \frac{1}{\alpha_s(\mu)} f_k^{(0)}(\lambda) + f_k^{(1)}(\lambda, Q, \mu) + f'_k(\lambda, \alpha_s) \quad (13)$$

where

$$\lambda = b_0 \alpha_s(\mu^2) \ln \bar{N} \quad (14)$$

The functions $f_k^{(0)}(\lambda)$, $f_k^{(1)}(\lambda)$ and $f'_k(\lambda)$, as well as $g_{abd}^{(1)}(\lambda)$ in Eq. (7), the exponent due to wide angle soft radiation, are all listed in Appendix A.

If one wishes to sum only threshold-enhanced logarithms, an easy modification of Eq. (7) [10, 17] suffices. One merely neglects the recoil term \mathbf{Q}_T in the kinematic factor in the third line of Eq. (7), upon which the \mathbf{Q}_T integral sets \mathbf{b} to zero.

Having reviewed the resummed cross section for the direct component of prompt photon production let us now turn to the fragmentation component. The joint-resummed expression

for the fragmentation component was derived in Refs. [10, 34]. It is given by

$$\begin{aligned}
\frac{p_T^3 d\sigma_{AB \rightarrow \gamma+X}^{(\text{frag})}}{dp_T} &= \sum_{abc} \frac{p_T^4}{8\pi S^2} \int_C \frac{dN}{2\pi i} f_{a/A}(N, \mu_F) f_{b/B}(N, \mu_F) D_{\gamma/c}(2(N-1) + 3, \mu_F) \\
&\times \int \frac{d^2 \mathbf{Q}_T}{(2\pi)^2} \Theta(\bar{\mu} - Q_T) \int d^2 \mathbf{b} e^{i\mathbf{b} \cdot \mathbf{Q}_T} \left(\frac{S}{4|\mathbf{p}_T - \mathbf{Q}_T/2|^2} \right)^{N+1} \\
&\times \int_0^1 d\tilde{x}_T^2 (\tilde{x}_T^2)^N \frac{|M_{ab \rightarrow cd}(\tilde{x}_T^2)|^2}{\sqrt{1 - \tilde{x}_T^2}} C_{ab \rightarrow cd}(\alpha_s(\mu), \tilde{x}_T^2) \\
&\times \exp \left[E_{ab \rightarrow cd} \left(N, b, \frac{4p_T^2}{\tilde{x}_T^2}, \mu_F \right) \right]. \tag{15}
\end{aligned}$$

Here $D_{\gamma/c}(2(N-1) + 3, \mu_F)$ is the fragmentation function which expresses the probability of parton c fragmenting into a photon. To include the soft-collinear effects we shall now make modifications similar to those for the direct component. There is however an important difference associated with the fragmentation function, which we shall discuss further below. Soft-collinear effects due to radiation from initial state partons a and b , can again be included by replacing the parton distribution functions by the functions $\mathcal{C}_{i/A}(Q, b, N)$ and $\mathcal{C}_{j/B}(Q, b, N)$, and then of course modifying the associated exponent functions accordingly. To include the soft-collinear effects due to radiation from parton d , we shall modify the final state exponent as in Eq. (13). Finally, for parton c , associated with the fragmentation function, one could envisage two approaches. In the first, one can include the soft-collinear effects directly via a modified exponent function, in analogy to the treatment for parton d . This is the approach we shall study numerically in section 3. In a second approach one could attempt to include them instead through evolution, in analogy to partons a and b . We discuss this approach, which is problematic, further in appendix C.

The modification required for the first approach is derived as follows [17, 35, 36]. Starting with the usual integral form for the initial state exponent in threshold resummation [37, 38]

$$E_c^{\text{PT}}(N, Q) = 2 \int_0^1 dz \frac{z^{N-1} - 1}{1 - z} \int_{\mu_F}^{Q(1-z)} \frac{d\mu}{\mu} A(\alpha_s(\mu)) \tag{16}$$

one replaces, for a final state fragmenting (anti)quark,

$$\frac{z^{N-1} - 1}{1 - z} \longrightarrow \frac{z^{N-1} - 1}{1 - z} - z^{N-1}. \tag{17}$$

As a consequence, carrying out the integral, one finds

$$E_c^{\text{PT}}(N, Q, \mu, \mu_F) = E_c^{\text{PT,eik}}(N, Q, \mu, \mu_F) + E_c^{\text{PT,SC}}(N, Q), \tag{18}$$

where the first term contains the leading and next-to-leading threshold logarithms, and the second term the leading soft-collinear effects. The result is

$$E_c^{\text{PT,eik}}(N, Q, \mu, \mu_F) = \frac{1}{\alpha_s(\mu)} q^{(0)}(\lambda) + q^{(1)}(\lambda), \tag{19}$$

where $\lambda = b_0 \alpha_s \ln \bar{N}$. The functions $q^{(0,1)}(\lambda)$ are defined in appendix A. For the soft-collinear effects we find

$$E_c^{\text{PT,SC}}(N, Q) = -\frac{A^{(1)}}{2\pi b_0} \exp \left(-\frac{\lambda}{b_0 \alpha_s} \right) \left[\ln(1 - 2\lambda) \right]. \tag{20}$$

We now arrive at the expression

$$\begin{aligned}
\frac{p_T^3 d\sigma_{AB \rightarrow \gamma+X}^{(\text{frag})}}{dp_T} &= \sum_{abc} \frac{p_T^4}{8\pi S^2} \int_{\mathcal{C}} \frac{dN}{2\pi i} D_{\gamma/c}(2(N-1)+3, \mu_F) \\
&\times \int \frac{d^2 \mathbf{Q}_T}{(2\pi)^2} \int d^2 \mathbf{b} e^{i\mathbf{b} \cdot \mathbf{Q}_T} \Theta(\bar{\mu} - Q_T) \left(\frac{S}{4\mathbf{p}_T'^2} \right)^{N+1} \\
&\times \mathcal{C}_{i/A}(Q, b, N) \mathcal{C}_{j/B}(Q, b, N) \Sigma_{ab \rightarrow cd}^{(\text{resum})}(N-1, b) . \tag{21}
\end{aligned}$$

Here, $\Sigma_{ab \rightarrow cd}^{(\text{resum})}(N, b)$ is the resummed cross section for the partonic process $ab \rightarrow cd$ in combined N, b space and reads

$$\begin{aligned}
&\Sigma_{ab \rightarrow cd}^{(\text{resum})}(N-1, b) \\
&= \exp \left[E_a^{\text{PT}}(N, b, Q, \mu) + E_b^{\text{PT}}(N, b, Q, \mu) + E_c^{\text{PT}}(N, Q, \mu, \mu_F) + F_d(N, Q, \mu) \right] \\
&\times \text{Tr} \left\{ H(Q, \mu) \bar{\text{P}} \exp \left[\int_{p_T}^{p_T/N} \frac{d\mu'}{\mu'} \Gamma_S^\dagger(\alpha_s(\mu')) \right] S \left(\alpha_s \left(\frac{p_T}{N} \right) \right) \right. \\
&\times \text{P} \exp \left[\int_{p_T}^{p_T/N} \frac{d\mu'}{\mu'} \Gamma_S(\alpha_s(\mu')) \right] \left. \right\} . \tag{22}
\end{aligned}$$

Here $E_a^{\text{PT}}(N, b, Q, \mu)$, $E_b^{\text{PT}}(N, b, Q, \mu)$ correspond to Eq. (8), $F_d(N, Q, \mu)$ to Eq. (13) and $E_c^{\text{PT}}(N, Q, \mu, \mu_F)$ to Eq. (18). The exponents inside the trace are associated with wide angle soft radiation and its form is discussed below.

The expression for the resummed exponent differs crucially from the corresponding expression for the direct component in that there are a larger number of color structures that can connect the external partons in (5) as opposed to direct production. This requires a set of corresponding coefficient functions and soft anomalous dimension matrices, which may mix under soft emissions. These have already been computed for the threshold-resummation studies of [18, 34]. In appendix B we recall the derivation of these factors. As a well-known result of this mixing of different color structures the radiative factor for wide angle soft radiation takes the form of a matrix in the space of allowed tensors that connect the color representations of partons a, b, c, d into a singlet. The trace in Eq. (22) is taken in that color tensor space. S is a soft gluon function that represents non-collinear soft gluon emission, while H is the hard scattering function describing the short distance hard scattering. Both H and S are matrices in color tensor space. At lowest order, $S_{LI} = \text{Tr}[c_L^\dagger c_I]$ where c_L^\dagger and c_I are color tensors [39]. The soft anomalous dimension matrix Γ_S represents the evolution of the soft function from scale p_T/N to p_T . The symbols P and $\bar{\text{P}}$ denote path ordering in the space of color tensors.

Clearly, in a color basis in which the soft anomalous dimension Γ_S is diagonal, the path-ordered exponentials of matrices in Eq. (22) reduce to a sum of simple exponentials. Expressions for these soft anomalous dimension matrices have been given in Ref. [39] in terms of the mandelstam invariants s, t, u associated with the $2 \rightarrow 2$ kinematics of reactions (4) and (5). In the threshold limit $\hat{x}_T^2 \rightarrow 1$ one can approximate these invariants in the soft anomalous dimension matrices by

$$s \rightarrow 4p_T^2, \quad t \rightarrow -2p_T^2, \quad u \rightarrow -2p_T^2 . \tag{23}$$

We will illustrate this diagonalization procedure for the case of $qq \rightarrow qq$ in Appendix B. After the diagonalization procedure is carried out, the resummed exponent for a given partonic channel is given by [18]

$$\begin{aligned} \Sigma_{ab \rightarrow cd}^{(\text{resum})}(N-1, b) &= C_{ab \rightarrow cd} \exp \left[E_a^{\text{PT}}(N, b, Q, \mu) + E_b^{\text{PT}}(N, b, Q, \mu) \right. \\ &\quad \left. + E_c^{\text{PT}}(N, Q, \mu, \mu_F) + F_d(N, Q, \mu) \right] \\ &\times \left[\sum_I G_{ab \rightarrow cd}^I \exp \left(\Gamma_{ab \rightarrow cd}^{I,(\text{int})}(N) \right) \right] \sigma_{ab \rightarrow cd}^{(\text{Born})}(N-1, b) \end{aligned} \quad (24)$$

The sum runs over all possible color configurations I with $G_{ab \rightarrow cd}^I$ representing a weight for each color configuration such that $\sum_I G_{ab \rightarrow cd}^I = 1$. The anomalous dimensions $\Gamma_{ab \rightarrow cd}^{I,(\text{int})}(N)$ are given by

$$\Gamma_{ab \rightarrow cd}^{I,(\text{int})}(N) = \int_0^1 \frac{z^{N-1} - 1}{1-z} D_{I,ab \rightarrow cd} \left(\alpha_s \left((1-z)^2 Q^2 \right) \right) \quad (25)$$

The NLL expansion of $\Gamma_{ab \rightarrow cd}^{I,(\text{int})}(N)$ is given by

$$\Gamma_{ab \rightarrow cd}^{I,(\text{int})}(N) = \frac{D_{I,ab \rightarrow cd}^{(1)}}{2\pi b_0} \ln(1-2\lambda) + O \left(\alpha_s (\alpha_s \ln N)^k \right) \quad (26)$$

The coefficients $D_{ab \rightarrow cd}^{(1)}$, the color weights G^I , one loop hard coefficients $C_{ab \rightarrow cd}^{(1)}$ and Born cross sections in N -space $\Sigma_{ab \rightarrow cd}^{(\text{Born})}$ have been given in the Appendix of Ref. [34], for each of the partonic subprocesses in (5). Eqs. (21) and (24) are the expressions we used for the results in section 3.

Having presented the expressions for joint and threshold resummed production of prompt photons including soft-collinear effects, for both direct and fragmentation component, we next examine the latter numerically.

3 Numerical studies

In this section we study numerically the inclusion of the $\ln N/N$ terms for the case of prompt photon production for two kinematic conditions: those of $p\bar{p}$ collisions at the Tevatron at $\sqrt{S} = 1.96$ TeV [40,41], and those of the pN collisions in the E706 [42] fixed target experiment with $E_{\text{beam}} = 530$ GeV, corresponding to $\sqrt{S} = 31.5$ GeV. As in our previous study [17], we stress that our aim is primarily to assess the effect of such terms in relevant kinematic conditions, rather than perform a comprehensive comparison with data. Our assessments therefore mainly consist of comparing the same calculation with and without $\ln N/N$ terms, and compare this with the difference between LL and NLL accuracy.

Our default choices for various input parameters are as follows. We use joint resummation unless specified otherwise. We use the GRV parton density set [43], corresponding to $\alpha_s(M_Z) = 0.114$, with the evolution code of Ref. [44], changing flavor number at $\mu = m_c$ (1.4 GeV) and m_b (4.5 GeV). We choose the factorization and renormalization scale equal to p_T , and the non-perturbative parameter g_{NP} in Eq. (33) equal to 1 GeV^2 . For the

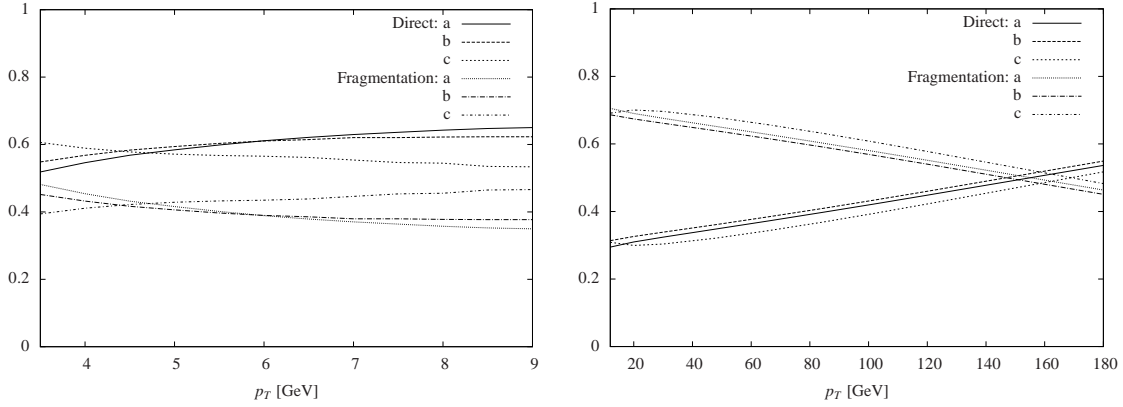


Figure 1: Relative contributions vs. p_T of direct and fragmentation photons for LL (a), NLL (b), NLL + $\ln N/N$ (c). The left pane shows the results for E706 kinematics and the right pane for Tevatron kinematics.

parameter χ we use the expression in Eq. (52), following [45], with $\eta = 1/4$. For our joint-resummed results, we chose for Tevatron (E706) kinematics the cut-off $\bar{\mu}$ in Eq. (10) equal to 15 (5) GeV. Regarding logarithmic accuracy, and unless stated otherwise, we refer to LL when using only $h_a^{(0)}$, $f_k^{(0)}$ and $q^{(0)}$, and $\bar{C}^{(ab \rightarrow \gamma d)} = \bar{C}^{(ab \rightarrow cd)} = 1$ (see Appendix A); we refer to NLL when also including $h_a^{(1)}$, $f_k^{(1)}$, $q^{(1)}$ and the virtual corrections discussed below Eq. (41). When including the soft-collinear $\ln N/N$ terms we use the full NLO anomalous dimension, evolved from scale μ_F to Q/χ in Eq. (46).

In Fig. 1 we show the relative contributions of the direct and fragmentation components for both kinematic conditions to the total result

$$\frac{\text{direct}}{\text{direct} + \text{fragmentation}}, \quad \frac{\text{fragmentation}}{\text{direct} + \text{fragmentation}}, \quad (27)$$

for LL, NLL, as well as NLL with soft-collinear effects. For E706 kinematics we observe that, as p_T increases, the contribution from the direct component becomes more dominant, but not such that the fragmentation component becomes wholly negligible. We note in particular that in the case of NLL with $\ln N/N$ the relative direct contribution decreases slightly over the range of p_T values.

In the case of Tevatron kinematics, for values of $p_T \leq 150$ GeV the relative direct contribution is larger than the relative fragmentation contribution. The contribution of soft-collinear effects is mostly larger than the difference between LL and NLL, the latter difference being quite small for joint resummation. In Fig. 2 we show the fragmentation component by itself for both kinematics, and for our three approximations. In the case of E706 kinematics we note that the NLL curve is decreased slightly relative to the LL curve. Furthermore, inclusion of the soft-collinear contribution leads to a further small decrease. In the case of Tevatron kinematics we see that the difference between the curves is even smaller, due to the smaller value of α_s at larger p_T values. Inclusion of the $\ln N/N$ terms lowers the result with respect to the NLL curve for p_T above 20 GeV by a few percent, but their contribution is negligible for p_T values above 110 GeV. In Fig. 3 we show a comparison between joint- and threshold resummation for both E706 and Tevatron kinematics. The curves are all relative to the joint NLL result without soft-collinear terms. While for E706 and joint resummation the inclusion

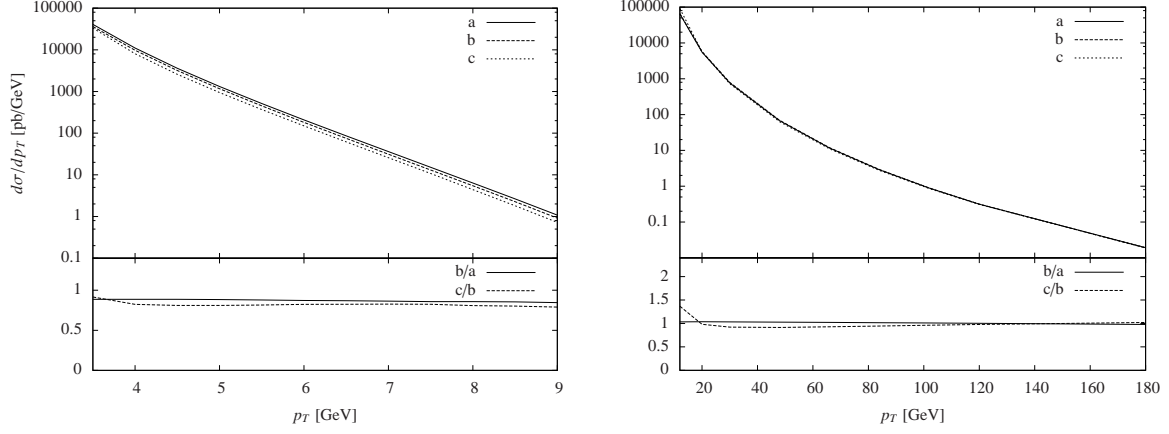


Figure 2: The LL (a), NLL (b) and NLL+ln N/N (c) calculations as well as the ratios NLL/LL, NLL+ln N/N /NLL vs. p_T . Left pane: E706, right pane: Tevatron.

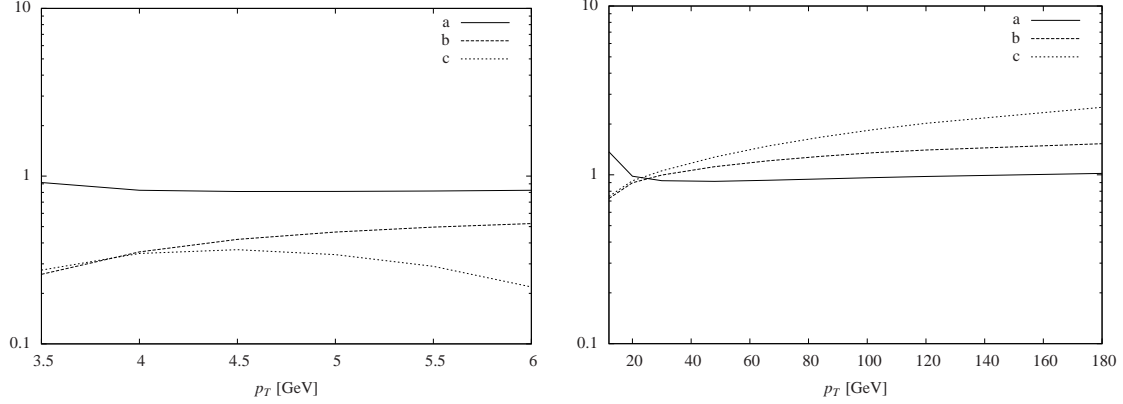


Figure 3: Comparison of joint resummation and threshold resummation effects, ratios to joint resummation NLL without ln N/N . The three curves show joint NLL with ln N/N (a), threshold NLL without ln N/N (b) and threshold NLL with ln N/N (c). Left pane: E706, right pane: Tevatron.

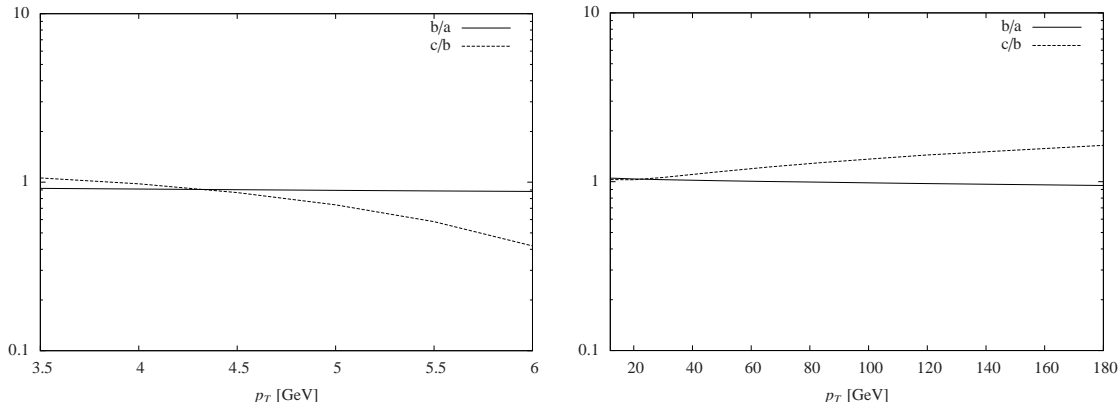


Figure 4: Same as the ratio plots in Fig. 2 but for threshold resummation. Left pane: E706, right pane: Tevatron.

of the $\ln N/N$ terms leads to only a small decrease of the NLL curve, we see that the effects are much more appreciable for threshold resummation. In particular we note that for p_T above 4 GeV the inclusion of $\ln N/N$ terms leads to a notable decrease of the NLL curve. This is very similar to what we found for the direct component in Ref. [17]. For Tevatron kinematics the inclusion of $\ln N/N$ terms for joint resummation is only appreciable for quite low values of p_T . For threshold resummation the situation is again notably different, with the inclusion of the soft-collinear terms leading to an appreciable increase relative to the pure NLL result, again in similarity to the direct component [17]. Finally, Fig. 4 is equivalent to the ratios shown in Fig. 2 but now for threshold resummation only. The soft-collinear terms change from increasing to decreasing the p_T distribution for E706 kinematics, with the opposite pattern occurring for Tevatron kinematics.

The behavior in Figs. 3 and 4 is quite similar to the direct case in our previous paper, which is perhaps not surprising since the resummation effects (LL, NLL and $\ln N/N$) are introduced by means of process independent exponentials and evolution of parton distribution functions. The extra contributions from the fragmentation parton and the additional color structures do not seem to change these patterns noticeably.

4 Conclusions

We have examined the effects of including terms of the form

$$\alpha_s^i \sum_j^{2i-1} d_{ij} \frac{\ln^j N}{N}. \quad (28)$$

in the production of a hard photon through fragmentation for p_T distributions at both collider and fixed target kinematics, at leading accuracy ($j = i$), both for joint and threshold resummation. This is the complement to an earlier study carried for the direct production component [17].

To the extent that leading terms of the form (28) arise from initial state radiation effects, we used the method of Refs. [32, 45] to include them. Those arising from final state emission we included both by extending the resummation exponents for the fragmenting parton and

the unobserved parton to leading $\ln N/N$ accuracy. As for the direct component, we found the combined $\ln N/N$ terms to be comparable to NLL corrections, and dependent on kinematics, either enhancing or suppressing. The contribution from $\ln N/N$ terms is noticable in the case of joint resummation although it remains small. This seems to imply that the corrections introduced by recoil effects tend to overshadow those of the soft-collinear terms. In the case of pure threshold resummation the soft-collinear effects play a more appreciable role. Overall we found a behavior comparable to the direct case studied previously.

Acknowledgments

We thank Daniel de Florian and Werner Vogelsang for helpful discussions. AM would like to thank Department of Atomic Energy-BRNS, India for financial support under the grant No. 2010/37P/47/BRNS. We would like to thank the Institute for Mathematical Sciences in Chennai for gracious hospitality. PM is grateful to the department of physics at Mumbai University for support during a visit. EL has been supported by the National Organization for Scientific Research (NWO), and the Foundation for Fundamental Research of Matter (FOM), program 104 “Theoretical Particle Physics in the Era of the LHC”. PM has been supported by the Bundesministerium für Bildung und Forschung (BMBF).

A Exponents

Here we list the exponents used in section 2. The initial state exponents for the LL and NLL case without inclusion of the $\ln N/N$ -terms are given by

$$h_a^{(0)}(\lambda, \beta) = \frac{A_a^{(1)}}{2\pi b_0^2} \left[2\beta + (1 - 2\lambda) \ln(1 - 2\beta) \right] \quad (29)$$

$$\begin{aligned} h_a^{(1)}(\lambda, \beta, Q, \mu, \mu_F) &= \frac{1}{2\pi b_0} \left(-\frac{A_a^{(2)}}{\pi b_0} + A_a^{(1)} \ln \left(\frac{Q^2}{\mu^2} \right) \right) \left[\frac{2\beta(1 - 2\lambda)}{(1 - 2\beta)} + \ln(1 - 2\beta) \right] \\ &+ \frac{A_a^{(1)} b_1}{2\pi b_0^3} \left[\frac{(1 - 2\lambda)(2\beta + \ln(1 - 2\beta))}{(1 - 2\beta)} + \frac{1}{2} \ln^2(1 - 2\beta) \right] \\ &- \frac{A_a^{(1)}}{\pi b_0} \lambda \ln \left(\frac{Q^2}{\mu_F^2} \right), \end{aligned} \quad (30)$$

while for the case when evolving the parton distribution functions down to Q/χ (Eq. (8)) they are

$$h_a^{(0)}(\beta) = \frac{A_a^{(1)}}{2\pi b_0^2} [2\beta + \ln(1 - 2\beta)] , \quad (31)$$

$$\begin{aligned} h_a^{(1)}(\beta, Q, \mu) &= \frac{A_a^{(1)} b_1}{2\pi b_0^3} \left[\frac{1}{2} \ln^2(1 - 2\beta) + \frac{2\beta + \ln(1 - 2\beta)}{1 - 2\beta} \right] + \frac{B_a^{(1)}}{2\pi b_0} \ln(1 - 2\beta) \\ &+ \frac{1}{2\pi b_0} \left[A_a^{(1)} \ln \left(\frac{Q^2}{\mu^2} \right) - \frac{A_a^{(2)}}{\pi b_0} \right] \left[\frac{2\beta}{1 - 2\beta} + \ln(1 - 2\beta) \right] . \end{aligned} \quad (32)$$

where $\beta = b_0 \alpha_s(\mu) \ln \chi$, and

$$A_a^{(1)} = C_a, \quad A_a^{(2)} = \frac{1}{2} C_a \left[C_A \left(\frac{67}{18} - \frac{\pi^2}{6} \right) - \frac{10}{9} T_R N_F \right] \quad (33)$$

with $C_q = C_F$ and $C_g = C_A$. Also we have

$$B_q^{(1)} = -\frac{3}{4} C_F, \quad B_g^{(1)} = -\pi b_0. \quad (34)$$

In these equations

$$b_0 = \frac{11C_A - 4T_R N_F}{12\pi}, \quad b_1 = \frac{17C_A^2 - 10C_A T_R N_F - 6C_F T_R N_F}{24\pi^2}. \quad (35)$$

where $T_R = 1/2$.

The functions $q^{(0,1)}(\lambda)$ in Eq. (19) are obtained by setting $\beta = \lambda$ in Eq. (29) and (30).

The final state exponents (13) involve the functions

$$f_a^{(0)} = -\frac{A_a^{(1)}}{2\pi b_0} [(1-2\lambda) \ln(1-2\lambda) - 2(1-\lambda) \ln(1-\lambda)] \quad (36)$$

$$\begin{aligned} f_a^{(1)} = & -\frac{A_a^{(1)} b_1}{2\pi b_0^3} [\ln(1-2\lambda) - 2\ln(1-\lambda) + \frac{1}{2} \ln^2(1-2\lambda) - \ln^2(1-\lambda)] \\ & + \frac{B_a^{(1)}}{2\pi b_0} \ln(1-\lambda) - \frac{A_a^{(2)}}{2\pi^2 b_0^2} [2\ln(1-\lambda) - \ln(1-2\lambda)] \\ & + \frac{A_a^{(1)}}{2\pi b_0} [2\ln(1-\lambda) - \ln(1-2\lambda)] \ln \frac{Q^2}{\mu^2} \end{aligned} \quad (37)$$

with $\lambda = b_0 \alpha_s(\mu) \ln \bar{N}$. Note that β only differs from λ for joint resummation; for threshold resummation $\beta = \lambda$. The final term in Eq. (13) reads

$$f'_q = \frac{A_q^{(1)}}{2\pi b_0} \exp\left(-\frac{\lambda}{\alpha_s b_0}\right) [\ln(1-2\lambda) - \ln(1-\lambda)], \quad (38)$$

$$f'_g = \frac{3A_g^{(1)}}{2\pi b_0} \exp\left(-\frac{\lambda}{\alpha_s b_0}\right) [\ln(1-2\lambda) - \ln(1-\lambda)]. \quad (39)$$

The wide-angle soft radiation exponents in Eq. (7) are

$$g_{q\bar{q}g}^{(1)}(\lambda) = -\frac{C_A}{\pi b_0} \ln(1-2\lambda) \ln 2, \quad g_{q\bar{q}q}^{(1)}(\lambda) = -\frac{C_F}{\pi b_0} \ln(1-2\lambda) \ln 2 \quad (40)$$

These expressions are obtained by expanding the perturbative functions $A_a(\alpha_s)$, $B_d(\alpha_s)$ and $D_{ab \rightarrow d\gamma}$ in powers of α_s

$$A_a(\alpha_s) = \frac{\alpha_s}{\pi} A_a^{(1)} + \left(\frac{\alpha_s}{\pi}\right)^2 A_a^{(2)} + O(\alpha_s^3). \quad (41)$$

The explicit forms of $C^{(ab \rightarrow \gamma d)}$ are shown in [4, 5]. The $C^{(ab \rightarrow cd)}$ are calculated by expanding the resummed cross section (Eq. (21)) to $\mathcal{O}(\alpha_s^3)$ and matching to the fixed order NLO result in [46]. We note that there is no factorization scale dependence in $h_a^{(1)}$ and the coefficient functions in Eq. (7) because of complete evolution from scale μ_F to Q/χ in Eqs. (14), (23) and (12).

B Diagonalization of soft anomalous dimensions

In this appendix we discuss the diagonalization procedure for the anomalous dimension matrices of Ref. [6] to arrive at the expressions of $G_{ab \rightarrow cd}^I$ and $D_{ab \rightarrow cd}^{(1)}$ of Ref. [34], which we also use here. In what follows, we illustrate this procedure for the partonic sub process $qq \rightarrow qq$ in the limit (23).

When one changes to a new color basis in which Γ_S is diagonal the resummed cross section takes a simpler form. The diagonalization procedure has been discussed in detail in Ref. [6]. Upon diagonalization the trace in Eq. (22) reduces to a simple sum of exponentials as in Eq. (24). The soft anomalous dimension matrix for the process $qq \rightarrow qq$ expressed in the t -channel singlet-octet basis is given by

$$\Gamma_{S'} = \frac{\alpha_s}{\pi} \begin{pmatrix} 2C_F U - \frac{1}{N_c}(T+U) & 2U \\ \frac{C_F}{N_c}U & 2C_F T \end{pmatrix} \quad (42)$$

where

$$U = \ln\left(-\frac{u}{s}\right) + i\pi, \quad T = \ln\left(-\frac{t}{s}\right) + i\pi. \quad (43)$$

This results in a slight difference from the initial state exponent in Ref. [18] which we are using. The difference for the partonic sub process $ab \rightarrow cd$ is then given by

$$\frac{\ln 2}{2} (C_a + C_b - C_c + C_d) \ln(1 - 2\lambda) \quad (44)$$

which we add to the diagonal terms of anomalous dimension matrix. This leads to

$$\Gamma_{S'} = \frac{\alpha_s}{\pi} \begin{pmatrix} -\frac{2}{3} & -2 \\ -\frac{4}{9} & -\frac{4}{3} \end{pmatrix} \ln 2. \quad (45)$$

The eigenvalues of this matrix (45) are $\lambda_1 = 0$ and $\lambda_2 = -2$, and the corresponding eigenvectors are, respectively

$$\begin{pmatrix} -3 \\ 1 \end{pmatrix}, \quad \begin{pmatrix} \frac{3}{2} \\ 1 \end{pmatrix}. \quad (46)$$

Now, we change the basis from t -channel singlet-octet basis to a new basis in which Γ_S is diagonal by using the matrix of eigenvectors

$$\mathcal{R}^{-1} = \begin{pmatrix} -3 & -\frac{3}{2} \\ 1 & 1 \end{pmatrix}. \quad (47)$$

Thus we obtain

$$\begin{aligned} & \text{Tr} \left\{ H(p_T, \mu) \bar{\text{P}} \exp \left[\int_{p_T}^{p_T/N} \frac{d\mu'}{\mu'} \Gamma_{S'}^\dagger(\alpha_s(\mu')) \right] \right. \\ & \quad \times S\left(\alpha_s\left(\frac{p_T}{N}\right)\right) \text{P} \exp \left[\int_{p_T}^{p_T/N} \frac{d\mu'}{\mu'} \Gamma_{S'}(\alpha_s(\mu'^2)) \right] \Big\} \\ & = \text{Tr} \left\{ \mathcal{R}^{-1} H(p_T, \mu) \mathcal{R} \mathcal{R}^{-1} \exp \left[\int_{p_T}^{p_T/N} \frac{d\mu'}{\mu'} \Gamma_S^\dagger \right] \mathcal{R} \mathcal{R}^{-1} S \exp \left[\int_{p_T}^{p_T/N} \frac{d\mu'}{\mu'} \Gamma_S^d \right] \mathcal{R} \right\} \end{aligned} \quad (48)$$

For the present case,

$$\Gamma_S^d = \mathcal{R}^{-1} \Gamma_{S'} \mathcal{R} = \begin{pmatrix} 0 & 0 \\ 0 & 2 \end{pmatrix} \quad (49)$$

H and S are the Mellin moments of 2×2 hard and soft matrices in color tensor space [6]. Substituting for them, one finds that the trace finally reduces to a sum of exponents

$$\hat{\sigma}_1 \exp \left[\frac{-\lambda_1 \ln 2}{2\pi b_0} \ln(1 - 2\lambda) \right] + \hat{\sigma}_2 \exp \left[\frac{-\lambda_2 \ln 2}{2\pi b_0} \ln(1 - 2\lambda) \right] \quad (50)$$

where $\hat{\sigma}_1$ and $\hat{\sigma}_2$ are $H'_{1i} S'_{i1}$ and $H'_{2i} S'_{i2}$ respectively, H' and S' being the hard and soft matrices in the new basis. Identifying $\frac{\hat{\sigma}_1}{\sigma_{born}}$ and $\frac{\hat{\sigma}_2}{\sigma_{born}}$ with $G_{qq \rightarrow qq}^1$ and $G_{qq \rightarrow qq}^2$ and $\frac{-\lambda_1 \ln 2}{2\pi b_0}$ and $\frac{-\lambda_2 \ln 2}{2\pi b_0}$ with $D_{qq \rightarrow qq}^1$ and $D_{qq \rightarrow qq}^2$, one obtains the relevant term in the exponent in Eq. (24).

C Soft-collinear effects in photon fragmentation function

In this appendix we discuss the possibility of including the leading soft-collinear effects in a manner exactly analogous to the initial state in [17], i.e. Q/\bar{N} . The present case is however special because the evolution equation for the photon fragmentation function is inhomogeneous.

To leading order, the non-singlet evolution equation for the photon fragmentation function $D_{\gamma/c}(N, \mu_F)$, where c is the parton that fragments into a photon, reads, in moment space

$$\frac{dD_{\gamma/c}(N, \mu^2)}{d \ln \mu^2} = \frac{\alpha}{2\pi} k^{(0)}(N) + \frac{\alpha_s(\mu^2)}{2\pi} P^{(0)}(N) D_{\gamma/c}(N, \mu^2) \quad (51)$$

where to $\mathcal{O}(1/N)$, for 3 active flavors

$$k^{(0)}(N) = \frac{4}{3N}, \quad P^{(0)}(N) = C_F \left(-2 \ln \bar{N} - \frac{1}{N} + \frac{3}{2} \right). \quad (52)$$

The inhomogeneous term arises because the photon, in contrast to hadrons, has a pointlike interaction with a quark. Correspondingly, the solution to Eq. (51) is the sum of a homogeneous (hadronic) and inhomogeneous (pointlike) part

$$D^\gamma(N, \mu^2) = D_{\text{had}}^\gamma(N, \mu^2) + D_{\text{pl}}^\gamma(N, \mu^2). \quad (53)$$

To leading logarithmic accuracy the homogeneous solution is

$$D_{\text{had}}^\gamma(N, \mu^2) = L^{-\frac{P^{(0)}(N)}{2\pi b_0}} D_{\text{had}}^\gamma(N, \mu_0^2) \quad (54)$$

where

$$L = \frac{\alpha_s(\mu^2)}{\alpha_s(\mu_0^2)} = 1 - b_0 \alpha_s(\mu_0^2) \ln \left(\frac{\mu^2}{\mu_0^2} \right) \quad (55)$$

To see what evolution from Q to Q/\bar{N} corresponds to, we substitute $\mu_0 = Q$ and $\mu = Q/\bar{N}$ and find

$$\begin{aligned} L^{-\frac{P^{(0)}(N)}{2\pi b_0}} &= \left(1 + 2b_0 \alpha_s \ln(\bar{N}) \right)^{\frac{1}{\pi b_0} C_F (\ln(\bar{N}) + \frac{1}{2N} - \frac{3}{4})} \\ &\simeq \exp \left(\frac{\alpha_s C_F}{\pi} \left[2 \ln^2(\bar{N}) + \frac{\ln(\bar{N})}{N} - \frac{3}{2} \ln(\bar{N}) \right] \right) \end{aligned} \quad (56)$$

which indeed sums the leading soft-collinear effects.

We now discuss the point-like (inhomogeneous) solution to Eq. (51). To LL accuracy it reads

$$D_{\text{pl}}^\gamma(N, \mu^2) = \frac{4\pi}{\alpha_s} \left[1 - L^{1 - \frac{P^{(0)}(N)}{2\pi b_0}} \right] \frac{1}{1 - \frac{P^{(0)}(N)}{2\pi b_0}} \frac{\alpha}{8\pi^2 b_0} k^{(0)}(N). \quad (57)$$

Notice that $D_{\text{pl}}^\gamma(N, \mu_0^2) = 0$, and that it is indeed proportional to $1/N$ via $k^{(0)}(N)$, see Eq. (52). For $\mu_0 = Q$ and $\mu = Q/\bar{N}$ the factor in square brackets can be rewritten as follows

$$\left[1 - L^{1 - \frac{1}{2\pi b_0} P^{(0)}(N)} \right] = \left[L^{\frac{P^{(0)}(N)}{2\pi b_0}} - (1 + 2b_0\alpha_s \ln(\bar{N})) \right] L^{-\frac{P^{(0)}(N)}{2\pi b_0}}. \quad (58)$$

We can rewrite the contents of square brackets as

$$\begin{aligned} & 1 - \frac{\alpha_s C_F}{\pi} \left[2 \ln^2(\bar{N}) + \frac{\ln(\bar{N})}{N} - \frac{3}{2} \ln(\bar{N}) \right] - (1 + 2b_0\alpha_s \ln(\bar{N})) \\ &= -\frac{\alpha_s}{\pi} \left[2C_F \ln^2(\bar{N}) + C_F \frac{\ln(\bar{N})}{N} - \frac{3}{2} C_F \ln(\bar{N}) + 2\pi b_0 \ln(\bar{N}) \right]. \end{aligned} \quad (59)$$

The expression in Eq. (57) then becomes

$$\begin{aligned} D_{\text{pl}}^\gamma \left(N, \frac{Q^2}{\bar{N}^2} \right) = & \left(\frac{-4 \left[2C_F \ln^2(\bar{N}) + C_F \frac{\ln(\bar{N})}{N} - \frac{3}{2} C_F \ln(\bar{N}) + 2\pi b_0 \ln(\bar{N}) \right]}{1 + \frac{C_F}{\pi b_0} (\ln(\bar{N}) + \frac{1}{2N} - \frac{3}{4})} \frac{\alpha}{8\pi^2 b_0} k^{(0)}(N) \right) L^{-\frac{P^{(0)}(N)}{2\pi b_0}} \end{aligned} \quad (60)$$

Carrying out the division inside the brackets for large N yields

$$D_{\text{pl}}^\gamma(N) = -\frac{\alpha}{\pi} \ln(\bar{N}) k^{(0)}(N) L^{-\frac{P^{(0)}(N)}{2\pi b_0}}. \quad (61)$$

Taken together the photonfragmentation function takes the form

$$D^\gamma \left(N, \frac{Q^2}{\bar{N}^2} \right) = D_{\text{had}}^\gamma \left(N, \frac{Q^2}{\bar{N}^2} \right) - \frac{4}{3} \frac{\alpha}{\pi} \frac{\ln(\bar{N})}{N} L^{-\frac{P^{(0)}(N)}{2\pi b_0}}. \quad (62)$$

Let us now perform a rough assessment of the validity of this approach to include soft-collinear effects. As the hadronic component of the photon fragmentation function has the property that one can sum the leading $\ln N/N$ effects through evolution, we factor it out of the full solution in (62), and estimate the large N behavior of the remainder based on a reasonable assumption of the non-perturbative N -dependence. We parametrize the hadronic part (stemming from the light quark flavors) in this limit as in Ref. [47] by $D_{\text{had}} \sim k_1 x^{-0.3} (1-x)^2 + k_2 \sqrt{x} (1.703 - x)$. It is now straightforward to show, after a Mellin transform, that the term for the point-like part contributes effectively at large N by a multiplicative factor

$$1 + \alpha_s (C \ln \bar{N} + \frac{C'}{N} \ln \bar{N}) \quad (63)$$

to the hadronic component for some constants C, C' . This affects the leading $\ln N/N$ term in (56), and would therefore seem to make this approach problematic.

References

- [1] G. Sterman, Nucl. Phys. **B281**, 310 (1987).
- [2] S. Catani and L. Trentadue, Nucl. Phys. **B327**, 323 (1989).
- [3] E. Laenen, G. Oderda and G. F. Sterman, Phys.Lett. **B438**, 173 (1998), [hep-ph/9806467].
- [4] S. Catani, M. L. Mangano and P. Nason, JHEP **9807**, 024 (1998), [hep-ph/9806484].
- [5] S. Catani, M. L. Mangano, P. Nason, C. Oleari and W. Vogelsang, JHEP **9903**, 025 (1999), [hep-ph/9903436].
- [6] N. Kidonakis and J. F. Owens, Phys. Rev. **D61**, 094004 (2000), [hep-ph/9912388].
- [7] P. Bolzoni, S. Forte and G. Ridolfi, Nucl. Phys. **B731**, 85 (2005), [hep-ph/0504115].
- [8] T. Becher and M. D. Schwartz, JHEP **1002**, 040 (2010), [0911.0681].
- [9] E. Laenen, G. F. Sterman and W. Vogelsang, Phys.Rev.Lett. **84**, 4296 (2000), [hep-ph/0002078].
- [10] E. Laenen, G. F. Sterman and W. Vogelsang, Phys.Rev. **D63**, 114018 (2001), [hep-ph/0010080].
- [11] G. Sterman and W. Vogelsang, Phys. Rev. **D71**, 014013 (2005), [hep-ph/0409234].
- [12] H. nan Li, Phys. Lett. **B454**, 328 (1999), [hep-ph/9812363].
- [13] G. Sterman and W. Vogelsang, JHEP **02**, 016 (2001), [hep-ph/0011289].
- [14] G. Parisi, Phys. Lett. **B90**, 295 (1980).
- [15] L. Magnea and G. Sterman, Phys. Rev. **D42**, 4222 (1990).
- [16] T. O. Eynck, E. Laenen and L. Magnea, JHEP **0306**, 057 (2003), [hep-ph/0305179].
- [17] R. Basu, E. Laenen, A. Misra and P. Motylinski, Phys.Rev. **D76**, 014010 (2007), [0704.3180].
- [18] D. de Florian and W. Vogelsang, Phys. Rev. **D72**, 014014 (2005), [hep-ph/0506150].
- [19] E. Laenen, L. Magnea and G. Stavenga, Phys.Lett. **B669**, 173 (2008), [0807.4412].
- [20] E. Laenen, G. Stavenga and C. D. White, JHEP **0903**, 054 (2009), [0811.2067].
- [21] E. Laenen, L. Magnea, G. Stavenga and C. D. White, JHEP **1101**, 141 (2011), [1010.1860].
- [22] E. Gardi, E. Laenen, G. Stavenga and C. D. White, JHEP **1011**, 155 (2010), [1008.0098].
- [23] G. Grunberg and V. Ravindran, JHEP **0910**, 055 (2009), [0902.2702].
- [24] G. Grunberg, Phys.Lett. **B687**, 405 (2010), [0911.4471].

- [25] G. Grunberg, Nucl.Phys. **B851**, 30 (2011), [1101.5377].
- [26] S. Moch and A. Vogt, JHEP **0904**, 081 (2009), [0902.2342].
- [27] S. Moch and A. Vogt, JHEP **0911**, 099 (2009), [0909.2124].
- [28] A. Vogt, G. Soar, S. Moch and J. Vermaseren, PoS **DIS2010**, 139 (2010), [1008.0952].
- [29] G. Soar, S. Moch, J. Vermaseren and A. Vogt, Nucl.Phys. **B832**, 152 (2010), [0912.0369].
- [30] A. Vogt, Phys.Lett. **B691**, 77 (2010), [1005.1606].
- [31] A. Almasy, G. Soar and A. Vogt, JHEP **1103**, 030 (2011), [1012.3352].
- [32] A. Kulesza, G. Sterman and W. Vogelsang, Phys. Rev. **D69**, 014012 (2004), [hep-ph/0309264].
- [33] P. Mathews *et al.*, Pramana **63**, 1367 (2004).
- [34] D. de Florian and W. Vogelsang, Phys. Rev. **D71**, 114004 (2005), [hep-ph/0501258].
- [35] M. Kramer, E. Laenen and M. Spira, Nucl.Phys. **B511**, 523 (1998), [hep-ph/9611272].
- [36] S. Catani, D. de Florian, M. Grazzini and P. Nason, JHEP **0307**, 028 (2003), [hep-ph/0306211].
- [37] G. Sterman, Nucl. Phys. **B281**, 310 (1987).
- [38] S. Catani, M. L. Mangano, P. Nason and L. Trentadue, Nucl. Phys. **B478**, 273 (1996), [hep-ph/9604351].
- [39] N. Kidonakis, G. Oderda and G. Sterman, Nucl. Phys. **B531**, 365 (1998), [hep-ph/9803241].
- [40] D0, V. M. Abazov *et al.*, Phys. Lett. **B639**, 151 (2006), [hep-ex/0511054].
- [41] CDF, D. Acosta *et al.*, Phys. Rev. **D70**, 074008 (2004), [hep-ex/0404022].
- [42] Fermilab E706, L. Apanasevich *et al.*, Phys. Rev. **D70**, 092009 (2004), [hep-ex/0407011].
- [43] M. Gluck, E. Reya and A. Vogt, Eur. Phys. J. **C5**, 461 (1998), [hep-ph/9806404].
- [44] A. Vogt, Comput. Phys. Commun. **170**, 65 (2005), [hep-ph/0408244].
- [45] A. Kulesza, G. Sterman and W. Vogelsang, Phys. Rev. **D66**, 014011 (2002), [hep-ph/0202251].
- [46] F. Aversa, P. Chiappetta, M. Greco and J. P. Guillet, Nucl. Phys. **B327**, 105 (1989).
- [47] M. Gluck, E. Reya and A. Vogt, Phys. Rev. **D48**, 116 (1993).